applied sciences

MDPI

Article

Research on Constant Power Control Strategy of Pure Electric Excavator

Tong Guo, Tianliang Lin *, Qihuai Chen, Haoling Ren and Shengjie Fu

College of Mechanical Engineering and Automation, Huaqiao University, Xiamen 361021, China; guot@hqu.edu.cn (T.G.); 11025049@zju.edu.cn (Q.C.); rhl@hqu.edu.cn (H.R.); fsj@hqu.edu.cn (S.F.)
* Correspondence: ltl@hqu.edu.cn

Received: 9 September 2020; Accepted: 23 October 2020; Published: 28 October 2020

Abstract: Electric construction machinery can achieve zero emissions and be pollution free in the process of construction. In an electric excavator, to make full use of the output power of the power source, the output power of the electric motor (EM) should be absorbed by a hydraulic pump on the most attainable level. Therefore, constant power control is generally employed to achieve power matching between the power source and hydraulic pump. In this paper, considering the shortcomings of a single constant power point in a traditional load sensing system of electric construction machinery, combining the discharge characteristics of the li-ion battery and the overload capability of EM, a piecewise constant power control strategy is proposed to realize the organic unity of power and safety for a novel electric construction machinery power train system. The control strategy is verified by simulations and experiments. The results show that the system can not only satisfy the large power output but also ensure the normal and stable operation of the system when the electric excavator meets the heavy load through the piecewise constant power control. The proposed control strategy improves the dynamic performance of the system on the basis of ensuring the safety of the system.

Keywords: electric excavator; energy saving; constant power control; dynamic property; battery

1. Introduction

Traditional construction machinery driven by an internal combustion engine (ICE) has shortcomings of poor emission and high energy consumption [1]. The electric construction machinery uses the electric motor (EM) as a power source, which can achieve zero emission and no pollution in the process of construction [2,3]. However, the traditional electric excavator only uses the EM to replace the ICE and imitates the working mode of the traditional ICE-driven excavator, which does not give full play to the excellent speed regulation performance and strong overload capacity of the EM.

The electric power train system has been successfully applied in the automotive field. However, there are essential differences between the excavator and automobile in terms of the transmission mode, working characteristics, and working conditions. Therefore, the control of EM in an electric excavator needs to be redesigned according to the actual requirements of the excavator.

Currently, research on the electric excavator is limited [4], especially on the control of EM in an electric excavator. Some research on the EM driving technology used in hybrid power train systems has been carried out. Chen et al. studied the EM applied to the energy regeneration system for a hybrid hydraulic excavator. The EM and hydraulic accumulator were used to prolong the energy regeneration time. The torque control for EM, which realized pressure compensation for the throttle valve to ensure dynamic performance, was studied [5]. Wang et al. studied the power train control and energy flow management for a hybrid hydraulic excavator. The dynamic programming control method was used to optimize system parameters [6]. Xiao et al. studied the parameter matching method for a hybrid hydraulic excavator [7]. Chen et al. applied the dynamic programming algorithm to control the power

train system [8]. In a hybrid hydraulic excavator, even though the EM is used, the engine is still the main power unit. The EM is an auxiliary power source, which compensates the load fluctuation and stabilizes working points of ICE in a high-efficiency area. The working conditions, control method, as well as control target of the EM in the electric excavator and that of a hybrid hydraulic excavator are totally different. Therefore, the EM control mode in a hybrid power system is not suitable for a pure electric system.

In an excavator, in order to ensure that the hydraulic pump can effectively absorb the power from the power source, and to avoid shutting down of the ICE in case of severe speed reduction in heavy duty [9], the power matching control strategy according to the power output characteristics of the hydraulic pump should be used. In a traditional ICE-driven excavator, due to the limited response ability of the ICE, the power matching between the power source and hydraulic pump is achieved by adjusting the working point of constant power for a variable displacement pump through a proportional reduction valve [10–12]. In a traditional electric excavator, the EM is used to replace the ICE and simulate the speed regulation of the ICE. The power matching control is generally based on a traditional hydraulic excavator, which did not give full play to its excellent speed regulation performance and strong overload capacity [13–15]. Besides, in a traditional electric excavator, the constant power setting point of the load sensing pump of the traditional pure electric drive excavator should be lower than the rated power of the EM, and there will be no system overload and shutdown failures. However, the rated power of the EM should be larger, which increases the cost of the whole machine [8,16].

In an electric excavator, the EM is the main power source. The excellent overload capability of the EM can enable the EM to work under short-term overload, when encountering heavy duty load [17–19], and improve the maximum output power of the power train system, so as to improve the dynamic performance of the system [20,21]. The constant power control based on variable speed EM to improve power matching between EM and the hydraulic pump needs to be further considered.

However, because of the usage of a power battery as energy storage, different states of charge (SOC) and temperatures of the battery will affect the output characteristics of EM. Therefore, in an electric excavator, through variable speed control, the maximum output power of the hydraulic pump should be set according to the discharge characteristics of the current power battery pack, the operation status of the EM, and its driver, which will be immune to overload and shutdown of the power train system and other faults [22].

Currently, studies on power matching control of an electric excavator at home and abroad are limited. In this paper, in order to improve the transmission efficiency of EM and the hydraulic pump, considering the influence of SOC and temperature on the discharge characteristics of the battery, a piecewise constant power control strategy is proposed to realize the organic unity of power and safety of the novel electric construction machinery power system. The paper is organized as follows: Section 2. System structure; Section 3. Constant power control based on discharge characteristics of power battery, Section 4. EM overload constant power control, Section 5. Simulation research; Section 6. Experimental research; Section 7. Conclusions.

2. System Structure

In this paper, an 8-ton electric excavator is taken as the research object to carry out the power system power matching research. The system structure is given in Figure 1. In this system, an EM is used to drive the hydraulic pump. A Li-ion battery is adopted to power the EM through the inverter. During the working process, variable speed control is used for the EM to satisfy the flow requirement of the system.

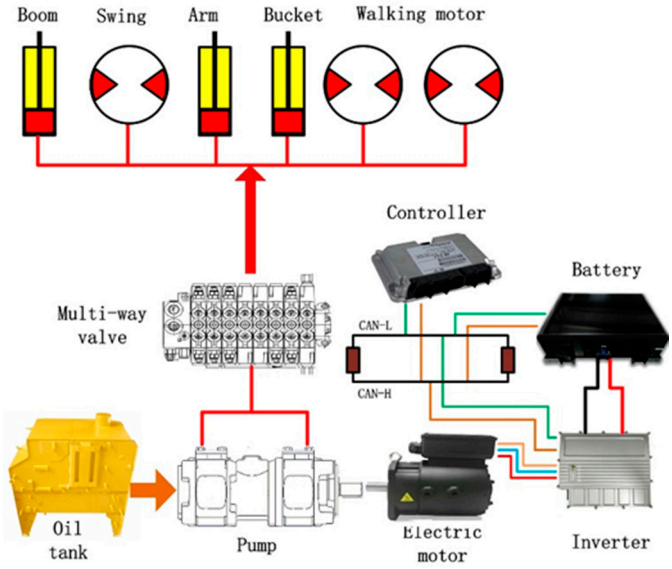

Figure 1. System structure.

The system schematic diagram can be given as Figure 2. As can be seen, an EM by variable speed control is applied to a fixed displacement pump to supply oil to the hydraulic system. A load sensing system hydraulic transmission system is employed. Maximum pressure of different loads is detected for EM control. The variable speed control to maintain the pressure drop of the throttle valve constant is used.

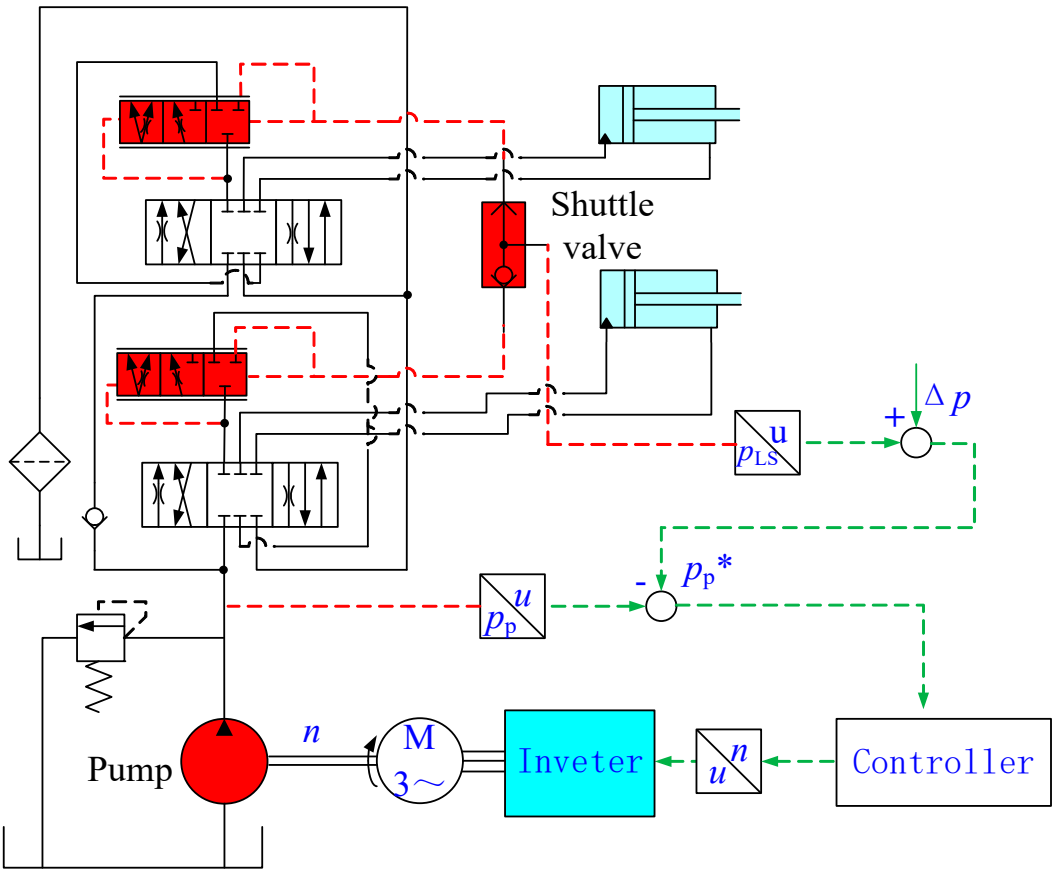

Figure 2. System schematic diagram.

Since the system parameter matching method is not directly related to the research carried out in this paper, this paper will not repeat, and only provides the basic parameters of the key components as follows. The parameters of EM can be given in Table 1:

Table 1. Parameters of the EM.

Type	Rated Power	Rated Torque	Rated Speed	Maximum Torque	Maxim Speed
PMSM	49 (kW)	260 (N·m)	1800 (rpm)	450 (N·m)	3000 (rpm)

The parameters of EM inverter can be given in Table 2:

Table 2. Parameters of the EM inverter.

Type	Rated Power	Rated Voltage	Voltage Range	Protection Level	Cooling
FOC	60 (kW)	510 (V)	350–710 (V)	IP67	Water

The parameters of power battery can be given in Table 3:

Table 3. Parameters of the power battery.

Type	Normal Energy	Normal Capacity	Maximum Discharge Current	Maximum Pulse Discharge Current	Voltage Range
LFP	117 (kW·h)	202 (A·h)	202 (A)	300 (A)	450–675 (V)

The hydraulic pump used is an internal gear pump and its displacement is 100 cc/r.

3. Constant Power Control Based on Discharge Characteristics of the Power Battery

As can be seen in Figure 3 which is provided by the battery manufacturer, the maximum discharge power of a cell monomer varies with the SOC at different ambient temperatures. Therefore, during the working process, the maximum discharge power of the battery should be limited according to the current environmental temperature and the SOC, so as to ensure that the battery will not over discharge and the battery life will not be shortened, and the system will run reliably due to the limitation of the discharge power.

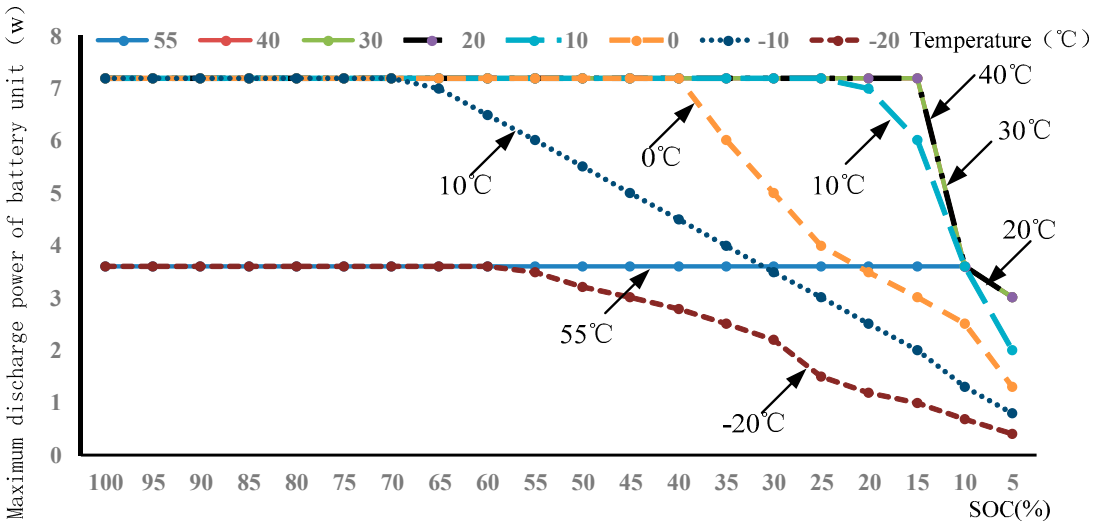

Figure 3. Maximum discharge power of the battery unit with SOC at different ambient temperatures.

The discharge capacity of the battery pack varies from different SOC. The larger the SOC, the stronger the discharge capacity and the larger the discharge power. The maximum allowable discharge power of the power li-ion battery can be measured through an experimental platform for different SOC and is given in Figure 4.

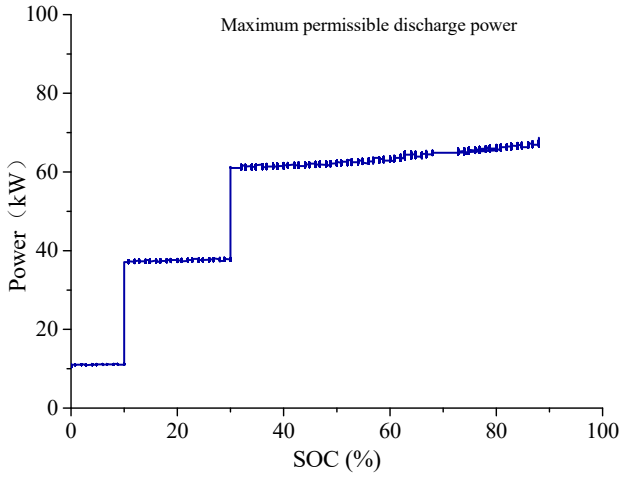

Figure 4. Maximum permissible discharge power of Li-ion batteries with different SOC 23 °C.

In the traditional electric excavator, by calculating the power required by the hydraulic pump, the output power of the battery is controlled. However, the discharge capacity of the power battery pack is also an important factor that should be taken into consideration. To avoid the over discharge of the battery pack and ensure control performance, the operating power of the power train system should be less than the maximum allowable discharge power of the battery pack. Therefore, during the control process, the current status information of the battery pack, such as SOC and temperature, should also be considered. The power of the control system should be not greater than the maximum allowable discharge power of the battery pack. The output power of the power train system can be described as:

$$P_p \leq P_{b\max} \cdot \eta_b \cdot \eta_{mc} \cdot \eta_m \cdot \eta_p, \quad (1)$$

where P_{bmax} is the maximum allowable discharge power of the current power lithium battery pack. η_b is the efficiency of the battery. η_{mc} is the efficiency of the EM driver. η_m is the efficiency of the EM. η_p is the efficiency of the hydraulic pump.

The total efficiency after converting to the output power of the hydraulic pump can be calculated according to:

$$\eta = \eta_b \cdot \eta_{mc} \cdot \eta_m \cdot \eta_p, \quad (2)$$

where, η is the total efficiency from the battery to the hydraulic pump.

As shown in Figure 5, the discharge efficiency of the power battery, which varies with different SOC, can be measured through an experimental platform and obtained according to the relationship between the discharge efficiency and the residual capacity of the battery measured during the discharge process at 23 °C from 100% to 10%.

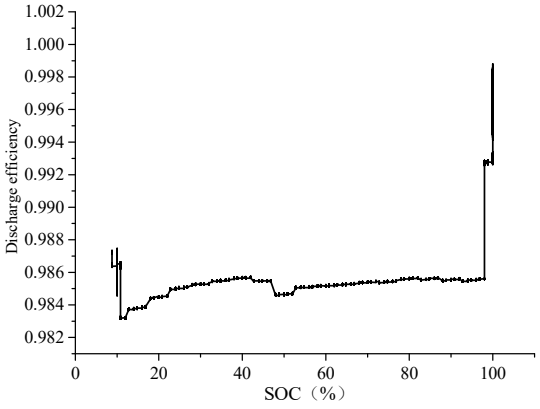

Figure 5. Discharge efficiency with SOC at 23 °C.

Considering the high efficiency of the EM inverter, the loss of the EM inverter can be neglected. According to Figure 5, the maximum allowable discharge power of the li-ion battery pack at 23 °C can be described as:

$$P_{b\max} = \begin{cases} 11 \ , & 0 \le SOC \le 10\% \\ 38 \ , & 10\% < SOC \le 30\%. \\ 63 \ , & 30\% < SOC \end{cases} \tag{3}$$

When the power of the system reaches the boundary constraint point of the output power, constant power control is needed to limit the output power of EM and to ensure the dynamic performance and the safety.

According to the current residual capacity of the power battery pack, the range of the power battery pack can be given as:

$$SOC_t \in (SOC_1, SOC_2), \tag{4}$$

where SOC_t is the real-time SOC. SOC_1 is the lower limit SOC of the maximum discharge power. SOC_2 is the upper limit SOC of the maximum discharge power.

The maximum allowable discharge power of the current power battery pack can be obtained through a battery management system (BMS). The maximum permissible output power of the current hydraulic pump can be calculated by Equation (1) and acquired as:

$$P_{p\max t} = P_{b\max t} \cdot \eta_b \cdot \eta_{mc} \cdot \eta_m \cdot \eta_p, \tag{5}$$

where P_{pmaxt} is the maximum permissible output power of the current hydraulic pumps. P_{bmaxt} is the maximum allowable output power of the current power battery pack.

When the required hydraulic pump power exceeds the maximum allowable output power of the current hydraulic pump, which can be described as:

$$P_p \ge P_{p\max t}, \tag{6}$$

where P_p is the power of the hydraulic pump.

At this time, the current output power of the hydraulic pump should be controlled based on the maximum allowable output power of the battery, which can be described as:

$$P_p = p_1 \cdot q_p = P_{p\max t}, \tag{7}$$

where p_1 is the output pressure of the pump. q_p is the output flow of the pump.

The current mechanical power of EM can be obtained as:

$$P_m = n_m \cdot T_m = P_{b\max t} \cdot \eta_b \cdot \eta_{mc} \cdot \eta_m, \tag{8}$$

where P_m is the output power of EM. n_m is the rotary speed of EM. T_m is the torque of EM.

The outlet pressure of the hydraulic pump can be given as:

$$\begin{cases} q_p = g(k, p_i) \\ p_1 = h(k, p_i, p_{LS}) \end{cases}, \tag{9}$$

where P_i is the pilot pressure. k is the pilot pressure adjustment coefficient. p_{LS} is the pressure of the maximum load.

Therefore, the output power of the hydraulic pump can be deduced as:

$$P_p = F(k, p_i, p_{LS}). \tag{10}$$

At this time, to ensure the maneuverability, the pilot pressure p_i should be adjusted to meet the demand of the speed v of the actuator and the flow q_p. Therefore, the pilot pressure p_i, the maximum load pressure p_{LS}, and the current maximum allowable output power p_{pmaxt} of the hydraulic pump can be used as input for control. The proportional coefficient k between the speed of the actuator and the pilot pressure can be obtained as:

$$k = F(P_{p\max t}, p_i, p_{LS}). \tag{11}$$

4. EM Overload Constant Power Control

When SOC of the battery pack is larger than 30%, the maximum allowable discharge power of battery is about 63 kW. The rated power of the EM is 49 kW. In order to improve the dynamic performance of the system, the EM can be operated above the rated power range in a short period of time. However, the overload operation of the EM will lead to a rapid increase of EM heat. Furthermore, the EM should also be operated within the maximum power range of EM. Therefore, in order to ensure the reliable operation of the power train system, the impact of the maximum allowable output power of the battery, the maximum power, and the temperature of the EM should be comprehensively considered in the constant power control.

The temperature curve of the stator of an EM measured with different load rates is given in Figure 6, which is provided by the EM manufacturer. As can be seen, the stator temperature of the EM increases with the increase of the load power. A permanent magnet synchronous motor (PMSM) has a higher power density, which easily leads to an excessive temperature rise in high-power operation. Excessive temperatures will lead to permanent magnet demagnetization or serious life degradation. Therefore, in the overload power mode, it is necessary to restrict the power according to the temperature of the EM.

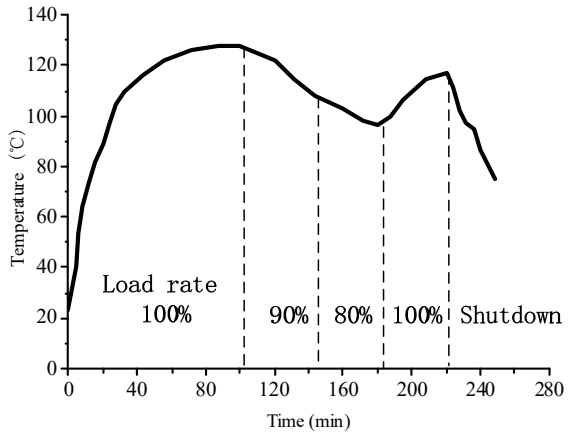

Figure 6. Temperature variation of an EM stator with load change.

As shown in Figure 7 and measured by an experimental platform, the temperature change of the EM driver before and after 2 min of operation at rated power is measured in the uncooled state. It can be seen that the temperature rise of the EM driver is large in case of the heavy duty load. The IGBT module is the key unit in the EM driver. Its current capacity decreases with the increase of temperature, which leads to a decrease of the driving ability of the EM driver. When the temperature rises to a certain extent, the failure rate will increase or even burst. Therefore, the working temperature of the EM driving system is another important factor affecting the dynamic performance and safety performance of the EM power train system.

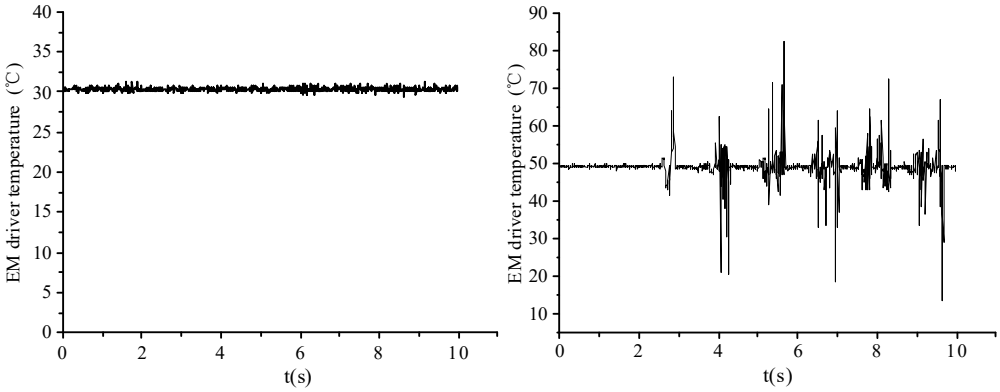

(**a**) EM driver temperature at start time (**b**) EM driver temperature after shutdown

Figure 7. EM driver temperature.

The IGBT module in the EM driver and permanent magnet in PMSM have their normal working temperature range. When their temperature reaches the critical temperature, constant power control should be employed to restrict the output power of the EM.

By modifying the proportional coefficient k between the system pressure drop and the pilot pressure, the system power is restrained, so as to reduce the temperature of the IGBT module of the EM driver and the permanent magnet of EM, so that it can operate in the allowable temperature range.

The constraints boundary of the temperature in the EM driver can be described as:

$$T_{pmc} < T_{pmc\max}, \tag{12}$$

where T_{pmc} is the working temperature of the EM driver. T_{pcmax} is the upper limitation of the EM driver.

The constraints boundary of the temperature in the EM can be described as:

$$T_{pm} < T_{pm\max}, \tag{13}$$

where T_{pm} is the working temperature of the EM. T_{pmmax} is the upper limitation of the EM.

In order to satisfy the dynamic performance of the power system, when the temperature of the EM and its driver is within the allowable range of normal operation, the output power of the hydraulic pump is limited, so that the current power of the EM does not exceed the maximum allowable power.

The constraints of overload constant power control can be expressed as:

$$\begin{cases} T_{pmc} < T_{pmc\max} \\ T_{pm} < T_{pm\max} \\ SOC \leq 30\% \end{cases}. \tag{14}$$

When the constraints of overload power constant power control are satisfied, the output power of the control hydraulic pump can be expressed as:

$$P_p \leq P_{mp} \cdot \eta_m \cdot \eta_p. \tag{15}$$

The maximum allowable output power of the pump can be described as:

$$P_{p\max t} = P_{b\max t}\eta_b \cdot \eta_{mc} \cdot \eta_m \cdot \eta_p. \tag{16}$$

When the required power of the hydraulic pump exceeds its maximum allowable output power, the current maximum power point substitution shown in Equation (11) and the current k can be acquired. After substituting the current k value into the closed-loop control, the EM drive system can work above the rated power under the premise of ensuring safety and improving the dynamic performance of the system.

When the temperature of the EM and its driver is detected to rise to the upper limit of the allowable temperature for its normal operation, the maximum allowable output power of the EM should be reduced by decrease the maximum allowable output power of the hydraulic pump. The maximum allowable discharge power of the battery pack can no longer be converted to the maximum allowable power of the EM as a reference standard.

The change trend of the temperature of EM and the motorist driver is the same. The driving ability of the EM driver decreases with the increase of temperature. When the temperature of the EM driver reaches the upper limit allowed by normal operation, the maximum allowable power of the EM should be reduced to the rated power at this time. The maximum allowable power of the EM cannot be pursued blindly.

The constraints of rated power constant power control can be expressed as:

$$T_{pmc} \geq T_{pmc\max} \text{ or } T_{pm} \geq T_{pm\max}. \tag{17}$$

When the constraints of constant power control of rated power are satisfied, the output power of the controlled hydraulic pump is as follows:

$$P_p \leq P_{me} \cdot \eta_m \cdot \eta_p. \tag{18}$$

The maximum allowable power of the pump output can be described as:

$$P_{p\max t} = P_{me} \cdot \eta_m \cdot \eta_p. \tag{19}$$

When the current required power of the hydraulic pump is greater than its maximum allowable output power, k can be adjusted according to Equation (11).

When the maximum allowable power of the power train system is reduced, the temperature of the EM and its driver cannot be reduced immediately. When the temperature reaches the critical point, if the maximum allowable power of the EM is rated, the power performance of the whole machine will be reduced.

Therefore, when the maximum allowable power of the EM is reduced from the peak power to the rated power, the temperature of the EM and its driver falls below a certain threshold, respectively, and can be described as:

$$T_{pm} \leq T_{pmb} \ \& \ T_{pmc} \geq T_{pmcb}, \tag{20}$$

where T_{pmb} is the threshold of the maximum allowable power of the motor rising from rated power to peak power. T_{pmcb} is the maximum allowable power of the EM riseing from the rated power to the temperature threshold of the peak power.

The overload power is reset to the maximum allowable power of the EM. When the current required power of the system is greater than the maximum allowable output power, the current maximum power point can be substituted into Equation (11) to determine the current k.

5. Simulation Research

To verify the feasibility of the control method, simulation research was carried out. Based on the variable speed control of EM and the load sensing hydraulic system, a constant power simulation model of variable pressure differential control was established by using AMESim simulation software platform, as shown in Figure 8. In this system, the hydraulic oil circuit is composed of a main oil circuit and pilot circuit. The main oil circuit drives the quantitative pump to supply oil through variable speed control of EM. On this basis, a load sensing system was constructed. The load simulation was carried out by the relief valve, which connects with the outlet of the control valve. The pilot oil circuit is controlled by the movement of the spool.

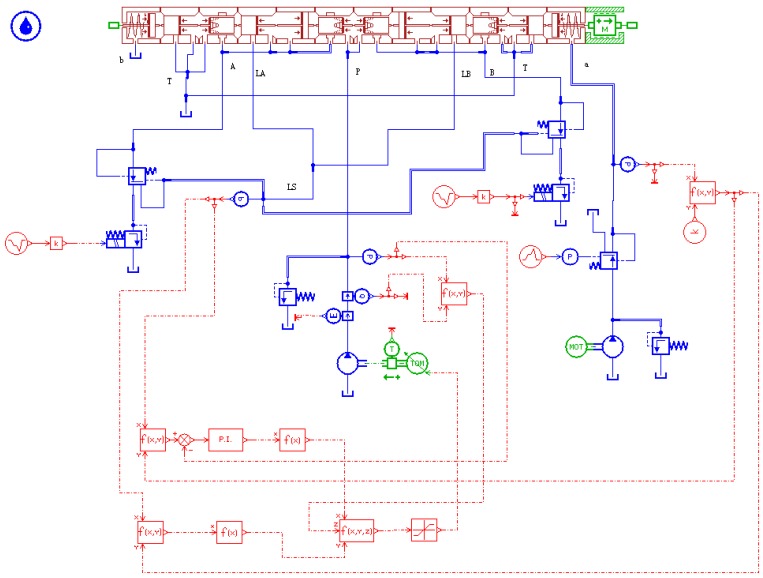

Figure 8. AMESim simulation model of constant power control.

The parameters of the components in the simulation model are given in Table 4.

Table 4. Parameters of components in the system.

Components	Value
Battery	Quantity of electricity: 117 kW·h. Capacity: 202 Ah
EM	Rated power: 49 kW. Rated torque: 260 N·m
EM driver	Voltage: 420–750 V. Maximum power: 63 kW
Hydraulic pump	Displacement: 100 mL/r. Pressure: 35 MPa
Controller	TTC60
Valve	Load sensing multi-way valve
Pilot pump	Displacement:10 mL/r. Pressure: 35 MPa
Pilot EM	Rated power: 2.5 kW
Auxiliary driver	Rated power: 5.5 kW. Output voltage: 380 V/24 V

The simulation model verifies that when the required power of the hydraulic pump is greater than its maximum allowable output power, the system pressure will be reduced, so as to make the pressure drop of the throttle valve change according to the outlet pressure of multi-way valves, the pilot pressure, and the maximum allowable output power of the hydraulic pump, which control the current output power of the hydraulic pump equal to its maximum allowable output power.

In the simulation model, the maximum allowable output power of the hydraulic pump is 20 kW and the simulation time is 20 s. The simulation curve of constant power control is given in Figure 9. The maximum load sensing pressure (LS pressure) and pilot pressure are set artificially. In the first

10 s, when the required power of the hydraulic pump does not reach the maximum allowable output power, the hydraulic pump outputs the power according to the load required power and maintains the pressure drop between the maximum load pressure and pump outlet pressure as the initial control target value. At this time, the pilot pressure and the ratio coefficient k are not limited by the maximum system power. In this paper, the initial set value of the k is 2:

$$\Delta p = kp_i, k = 2. \tag{21}$$

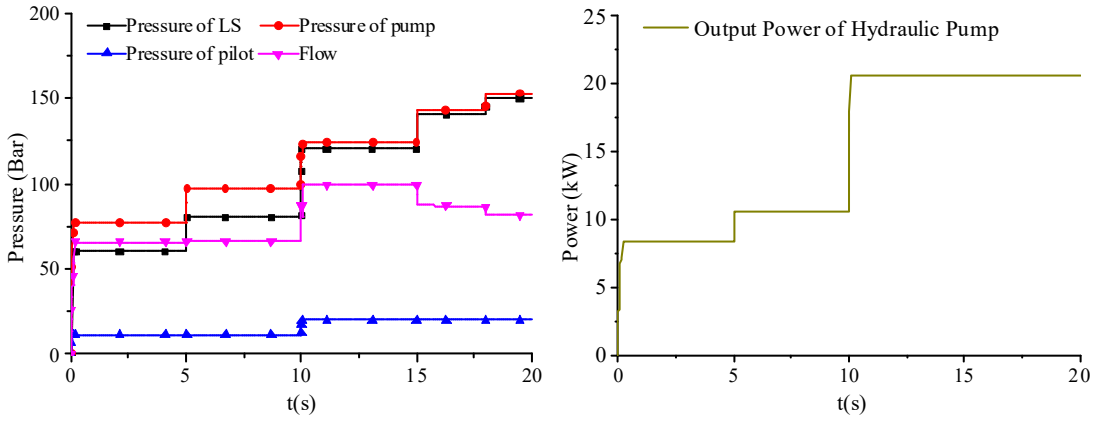

(**a**) Constant power pressure flow curve (**b**) Output power curve of hydraulic pump

Figure 9. Simulation results.

While, after 10 s of simulation, the current required power of the hydraulic pump reaches the maximum allowable output power. At this time, with the increase of the pump outlet pressure, the outlet flow of the hydraulic pump decreases, and the output power of the hydraulic pump equals the maximum allowable output power.

When the constant power point is reached, the pressure drop between the pump outlet pressure and the maximum load pressure, the pilot pressure, and the relationship between the ratio coefficient k no longer conform to Equation (20). The pilot pressure, the maximum load pressure, and the maximum allowable output power of the hydraulic pump are taken as the input values. The ratio coefficient is modified to change the differential drop of the system, so that the output power of the hydraulic pump is equal to the maximum allowable output power, which will not exceed the maximum allowable working range.

6. Experimental Research

Further experimental research on the proposed control strategy was carried out. The test platform is shown in Figure 10. The temperature of the EM and its driver was collected by a positive temperature coefficient (PTC) thermistor interface. The operation state of the power battery, including the maximum allowable discharge power, was collected by a CAN communication network through EM, EM inverter, and BMS. The relief valve was used for load simulation.

The state information of each component was transmitted to the controller of the whole machine. After calculation, the proportional coefficient k between the system pressure difference and the pilot pressure was obtained. Finally, combined with the pressure drop control, the piecewise constant power control was realized when the current required power of the hydraulic pump exceeded its maximum allowable output power.

Figure 10. Structure of the experimental platform.

During the test, the ambient temperature was 23 C. Because of the short test time, the battery temperature was unchanged. Firstly, the SOC of power battery was discharged to 10%, 30%, and 80%, respectively. The load was simulated by the proportional relief valve. In order to study the change of the system pressure drop conveniently, the pilot pressure was set as fixed.

Combined with Equation (3), the output of the power train system for different SOC are shown in Figures 11–13. The pressure–flow curves and output power curves of the hydraulic pump were obtained when the residual battery power is 10%, 30%, and 80%, respectively.

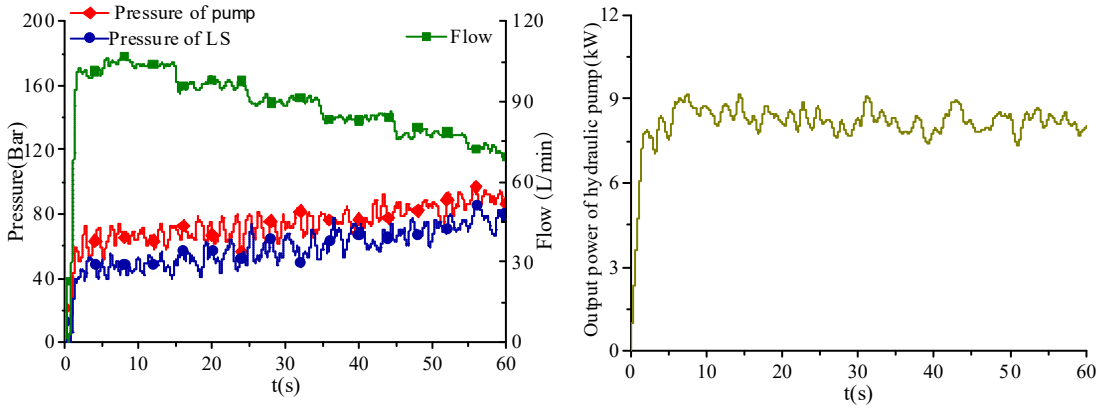

(**a**) Pressure-flow curve (**b**) Output power curve of hydraulic pump

Figure 11. Test curve at 10% SOC.

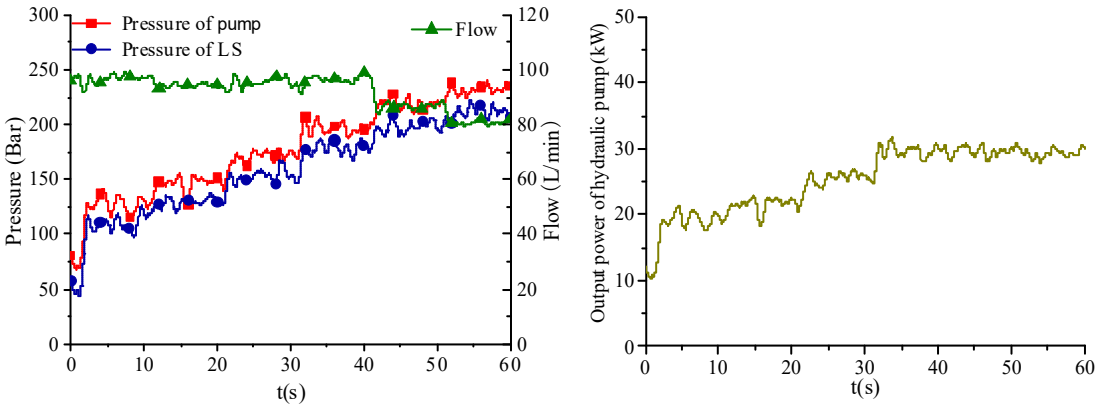

(**a**) Pressure-flow curve (**b**) Output power curve of hydraulic pump

Figure 12. Test curve at 30% SOC.

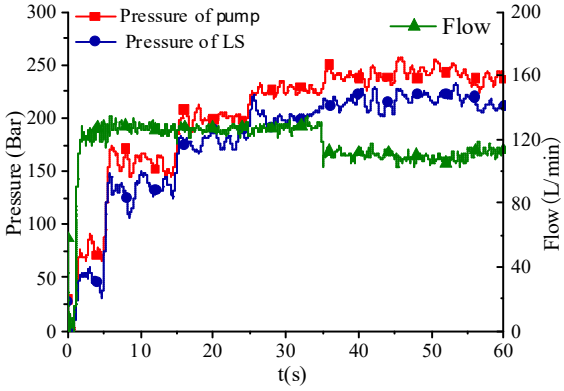

(**a**) Pressure-flow curve

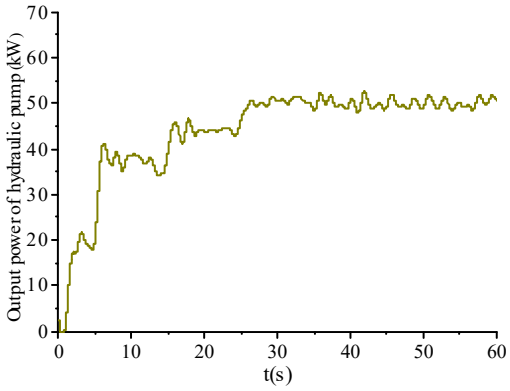

(**b**) Output power curve of hydraulic pump

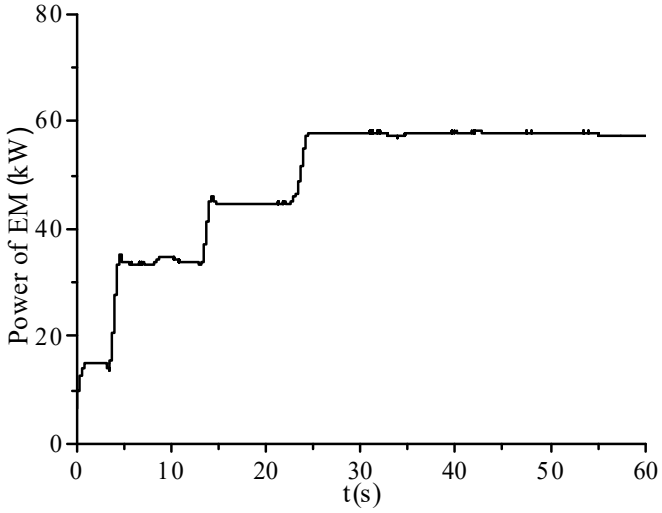

(**c**) Power of EM

Figure 13. Test curve at 30% SOC.

From the test results, it can be seen that when the discharge power of the power battery does not reach the maximum power at different stages of power supply, the output power increases with the increase of the load pressure, because the pressure drop and flow rate remain unchanged.

When the discharge power of the battery reaches the maximum allowable discharge power, namely, the output power of the hydraulic pump reaches the maximum allowable output power, the output power of the hydraulic pump no longer increases and remains constant. With the increase of the maximum load pressure, the flow rate of the hydraulic pump decreases and the pressure difference of the system decreases, and the output power of the hydraulic pump can be stabilized near the maximum allowable output power, so that the discharge power of the battery does not exceed the maximum allowable output power.

From the test results in Figure 12b, it can be seen that when SOC of the battery pack is more than 30% at room temperature, the latter half of the EM works in overload mode. Because the cooling effect of the water cooling system of the EM and its driver is superior, the temperature of the EM and its driver can hardly exceed the allowable working range, so the maximum power at this time is still the maximum power of the battery. The feasibility of piecewise constant power control can be further verified by the above experiments.

Compared with the constant power control of a single operation point, that is, the rated power of the li-ion battery is taken as the constant power, the piecewise constant power control strategy proposed in this paper can effectively ensure that the li-ion battery can avoid over discharge and

improve the service life of the power battery. In addition, it can also avoid that when the li-ion battery has a low SOC value, due to the insufficient power of battery can be provided for EM, the EM is stalled.

The single working point constant power control of s traditional electric excavator uses s lead-acid battery for power supply, without corresponding BMS. In this study, the power battery is a lithium-ion battery, which is equipped with a corresponding BMS unit. In the process of the constant power control experiment with a single operating point, when the battery SOC is low, the overload operation will cause the BMS to alarm continuously and then shut down. Therefore, the working condition of a single constant power working point cannot be reproduced. Although the experimental comparisons of these two control strategies are provided, through the research of this paper, based on the proposed control strategy, it can effectively ensure the reliable power supply of the power battery to the EM, and improve the reliability of the system.

7. Conclusions

In this paper, a piecewise constant power control strategy was proposed. The feasibility of the proposed control strategy was verified by simulation and experiment. According to the maximum allowable discharge power of battery at different temperatures and SOC, different maximum power points were set to control the power system with constant power, which satisfied the power performance and safety performance at the same time. According to the discharge capacity of the battery pack and the temperature of the EM as well as its driver, the strong overload capacity of the EM can be brought into play. Within the current discharge capacity of the power battery pack and the allowable range of the temperature of the EM and its driver, the EM can operate above the rated power to improve the dynamic performance of the system. When the working state of the battery and EM drive system is within the constraints, the maximum power point is reduced to ensure the safe and stable operation of the system.

By adopting the proposed control strategy for an electric excavator, in the case of heavy load, the system can not only meet the high-power output but also ensure the normal and stable operation of the system.

Author Contributions: T.G. proposed the idea of piecewise constant power control strategy. T.L. developed the structure and working mode. Q.C. wrote the paper. H.R. checked and edited the paper. S.F. analyzed the data. All authors have read and agreed to the published version of the manuscript.

Funding: The authors acknowledge the support of National Natural Science Foundation of China (51875218 & 51905180), Excellent Outstanding Youth Foundation of Fujian Province of China (2018J06014), Industry Cooperation of Major Science and Technology Project of Fujian Province of China (2019H6015) and Natural Science Foundation of Fujian Province of China (2018J01068&2019J01060), and STS project of Fujian Province of China (2018T3015). This work also has been supported by Hitachi Construction Machinery Co., Ltd.

Conflicts of Interest: The authors declare no conflict of interest.

Abbreviations

EM	Electric motor
ICE	Internal combustion engine
SOC	State of charge
BMS	Battery management system
PMSM	Permanent magnet synchronous motor
PTC	positive temperature coefficient
Δp	target pressure drop of throttle valve
$p_p{}^*$	target pressure of hydraulic pump
n	rotary speed of EM
P_p	power of hydraulic pump

q_p	output flow of pump
P_{bmax}	maximum allowable discharge power of the current power lithium battery pack
η_b	efficiency of the battery
η_{mc}	efficiency of the EM driver
η_m	efficiency of the EM
η_p	efficiency of the hydraulic pump
P_m	output power of EM
n_m	rotary speed of EM
T_m	torque of EM
P_i	pilot pressure
k	pilot pressure adjustment coefficient
p_{LS}	pressure of the maximum load
SOC_t	real time SOC
SOC_1	lower limit SOC of Maximum Discharge Power
SOC_2	upper limit SOC of Maximum Discharge Power
P_{pmaxt}	maximum permissible output power of the current hydraulic pumps
P_{bmaxt}	maximum allowable output power of the current power battery pack
T_{pmc}	working temperature of the EM driver
T_{pcmax}	upper limitation of the EM driver
T_{pmc}	working temperature of the EM
T_{pmmax}	upper limitation of the EM
T_{pmb}	threshold of the maximum allowable power of motor rising from rated power to peak power
T_{pmcb}	maximum allowable power of the EM rises from the rated power to the temperature threshold of the peak power

References

1. Kagoshima, M.; Komiyama, M.; Nanjo, T.; Tsutsui, A. Development of New Hybrid Excavator. *Kobelco Technol. Rev.* **2007**, 39–42.
2. Ge, L.; Quan, L.; Zhang, X.; Zhao, B.; Yang, J. Efficiency improvement and evaluation of electric hydraulic excavator with speed and displacement variable pump. *Energy Convers. Manag.* **2017**, *150*, 62–71. [CrossRef]
3. Huang, W.P.; Lin, T.L.; Ren, H.L.; Fu, S.; Chen, Q.; Zhou, S. Automatic Idle Speed Subdivision Control of Load Pressure Adaptation. *Chin. Hydraul. Pneum.* **2017**, *27*.
4. Lin, T.; Lin, Y.; Ren, H.; Chen, H.; Chen, Q.; Li, Z. Development and key technologies of pure electric construction machinery. *Renew. Sustain. Energy Rev.* **2020**, *132*, 110080. [CrossRef]
5. Chen, Q.; Lin, T.; Ren, H.; Fu, S. Novel potential energy regeneration systems for hybrid hydraulic excavators. *Math. Comput. Simul. (MATCOM)* **2019**, *163*, 130–145. [CrossRef]
6. Wang, H.; Wang, Q. Parameter Matching and Control of Series Hybrid Hydraulic Excavator based on Electro-hydraulic Composite Energy Storage. *IEEE Access* **2020**, *99*, 111899–111912. [CrossRef]
7. Xiao, Q.; Wang, Q. Parameter matching method for hybrid power system of hydraulic excavator. *China J. Highw. Transp.* **2008**, *21*, 121–126.
8. Chen, Q.; Lin, T.; Ren, H. Parameters optimization and control strategy of power train systems in hybrid hydraulic excavators. *Mechatronics* **2018**, *56*, 16–25. [CrossRef]
9. Zhang, J.; Zhang, T.; Cheng, L. Dynamic Simulation Research Based on AMESim Load-Sensing Pump. *Appl. Mech. Mater.* **2014**, *687*, 195–200. [CrossRef]
10. Yin, B.; Gao, D.; Sun, S.; Bo, X.; Hekun, J. Research on the Profile Design of Surface Texture in Piston Ring of Internal Combustion Engine. *J. Tribol.* **2018**, *140*, 61701.
11. Zavos, A.B.; Nikolakopoulos, P.G. Simulation of piston ring tribology with surface texturing for internal combustion engines. *Lubr. Sci.* **2015**, *27*, 151–176. [CrossRef]
12. Miao, J.; Guo, Z.; Yuan, C. Effect of Textured surface on the Friction Performance of Cylinder Liner-Piston Ring System in the Internal Combustion Engine. *Tribology* **2017**, *37*, 465–471.
13. Chen, Q.; Lin, T.; Ren, H. A novel control strategy for an interior permanent magnet synchronous machine of a hybrid hydraulic excavator. *IEEE Access* **2017**, *6*, 3685–3693.

14. Lin, T.; Huang, W.; Ren, H.; Fu, S.; Liu, Q. New compound energy regeneration system and control strategy for hybrid hydraulic excavators. *Autom. Constr.* **2016**, *68*, 11–20. [CrossRef]
15. Lin, T.; Chen, Q.; Ren, H.; Huang, W.; Chen, Q.; Fu, S. Review of boom potential energy regeneration technology for hydraulic construction machinery. *Renew. Sustain. Energy Rev.* **2017**, *79*, 358–371. [CrossRef]
16. Lin, T.; Wang, Q.; Hu, B.; Gong, W. Research on the energy regeneration systems for hybrid hydraulic excavators. *Autom. Constr.* **2010**, *19*, 1016–1026. [CrossRef]
17. Wang, D.; Zhang, D.; Xue, D.; Peng, C.; Wang, X. A New Hybrid Excitation Permanent Magnet Machine with Independent AC Excitation Port. *IEEE Trans. Ind. Electron.* **2018**, *66*, 5872–5882. [CrossRef]
18. Hoang, E. A New Structure of a Switching Flux Synchronous Polyphased Machine with Hybrid Excitation. In Proceedings of the 12th European Conference on Power Electronics and Applications (EPE2007), Aalborg, Denmark, 2–5 September 2007.
19. Mazlan, M.M.A.; Sulaiman, E.; Ahmad, M.Z.; Othman, S.M.N.S. Design optimization of single-phase outer-rotor hybrid excitation flux switching motor for electric vehicles. In Proceedings of the IEEE 2014 IEEE Student Conference on Research and Development (SCOReD), Penang, Malaysia, 16–17 December 2014; pp. 1–6.
20. Chen, Z.; Huang, F.; Yang, C.; Yao, B. Adaptive fuzzy backstepping control for stable nonlinear bilateral teleoperation manipulators with enhanced transparency performance. *IEEE Trans. Ind. Electron.* **2019**, *67*, 746–756. [CrossRef]
21. Liu, X.; Chen, H.; Zhao, J.; Belahcen, A. Research on the Performances and Parameters of Interior PMSM Used for Electric Vehicles. *IEEE Trans. Ind. Electron.* **2016**, *63*, 3533–3545. [CrossRef]
22. Lin, C.C.; Peng, H.; Grizzle, J.W.; Kang, J.M. Power management strategy for a parallel hybrid electric truck. *IEEE Trans. Control Systems Technol.* **2003**, *11*, 839–849.

Publisher's Note: MDPI stays neutral with regard to jurisdictional claims in published maps and institutional affiliations.

© 2020 by the authors. Licensee MDPI, Basel, Switzerland. This article is an open access article distributed under the terms and conditions of the Creative Commons Attribution (CC BY) license (http://creativecommons.org/licenses/by/4.0/).